

The first complete skeleton of *Megaloceros verticornis* (Dawkins, 1868) Cervidae, Mammalia, from Bilshausen (Lower Saxony, Germany): description and phylogenetic implications

Thekla Pfeiffer

With 5 figures and 4 tables

Abstract

The first well preserved, articulated skeleton of a young male deer of *Megaloceros verticornis* (Dawkins, 1868) was excavated from early Middle Pleistocene sediments of the clay pit of Bilshausen (Unter-Eichsfeld, Lower Saxony). This find made it possible, for the first time, to establish, using cladistic techniques, the systematic position of *Megaloceros verticornis* among Pleistocene and Holocene plesiometacarpal and telemetacarpal cervids. By contrast to the antler and tooth characters, the postcranial characters, in particular, are suitable for phylogeny reconstruction. *Megaloceros verticornis* from Bilshausen shows great similarity with *M. giganteus* of the Upper Pleistocene of Europe in its skeletal morphology, and bootstrap values (BP = 100) show strong support for the monophyly of *M. giganteus* and *M. verticornis*.

The analysis yields no evidence, however, of a close relationship between *Dama* and *Megaloceros*, which has been widely discussed in the literature because of the presence of large, palmated antlers in both genera.

Key words: Pleistocene, vertebrate palaeontology, cervids, *Megaloceros verticornis*, skeletal morphology, phylogeny reconstruction, cladistic analysis, taxonomy.

Zusammenfassung

Aus der Tongrube von Bilshausen (Unter-Eichsfeld, Niedersachsen) konnte das erste, vollständige Skelett eines jungen Hirsches von *Megaloceros verticornis* (Dawkins, 1868) aus mittelpleistozänen Sedimentablagerungen geborgen werden. Dieser Fund ermöglichte es erstmalig, die systematische Stellung von *Megaloceros verticornis* im System plesiometacarpaler und telemetacarpaler Hirsche des Pleistozäns und Holozäns auf breiter Basis zu untersuchen. Im Gegensatz zu den Geweih- und Zahnmerkmalen eignen sich die postcranialen Merkmale des Skelettes besonders gut für eine phylogenetische Rekonstruktion der Hirsche.

Die Gemeinsamkeit großer Schaufelgeweine bei *Dama dama* und dem Riesenhirsch *Megaloceros giganteus* hat dazu geführt, beide in eine enge phylogenetische Beziehung zu setzen, was in der Literatur zu einer anhaltenden Kontroverse geführt hat. Die Analyse der Morphologie der postcranialen Elemente zeigt jedoch, dass es keine enge Verwandtschaft zwischen *Dama* und *Megaloceros* gibt.

Schlüsselwörter: Pleistozän, Wirbeltierpaläontologie, Cerviden, *Megaloceros verticornis*, Skelettmorphologie, phylogenetische Rekonstruktion, kladistische Analyse, Taxonomie.

Introduction

In the early 20th century, Schmidt (1930, 1934) recovered a complete skeleton of *Alces latifrons* from the clay pit of Bilshausen (Lower Saxony, 20 km SE Göttingen), and several finds of articulated skeletal elements of large mammals were brought to light in the following years. In 1952 the complete extremities of another large cervid were found embedded in the clay, although the body was dislocated and destroyed. Scientific in-

vestigations ceased during the second world war, and some material was lost, but fortunately the best preserved find of the early years, the articulated skeleton of *A. latifrons*, was later discovered in the Museum of the Institute for Palaeontology at the University of Göttingen.

This museum also houses the well preserved skeleton of a young male deer of *Megaloceros verticornis* from Bilshausen (Fig. 1) excavated by D. Meischner and J. Schneider (both at the University of Göttingen) in November 1964

¹ Gutswiese 21, D-38162 Cremlingen, Germany.

Received April, accepted July 2002

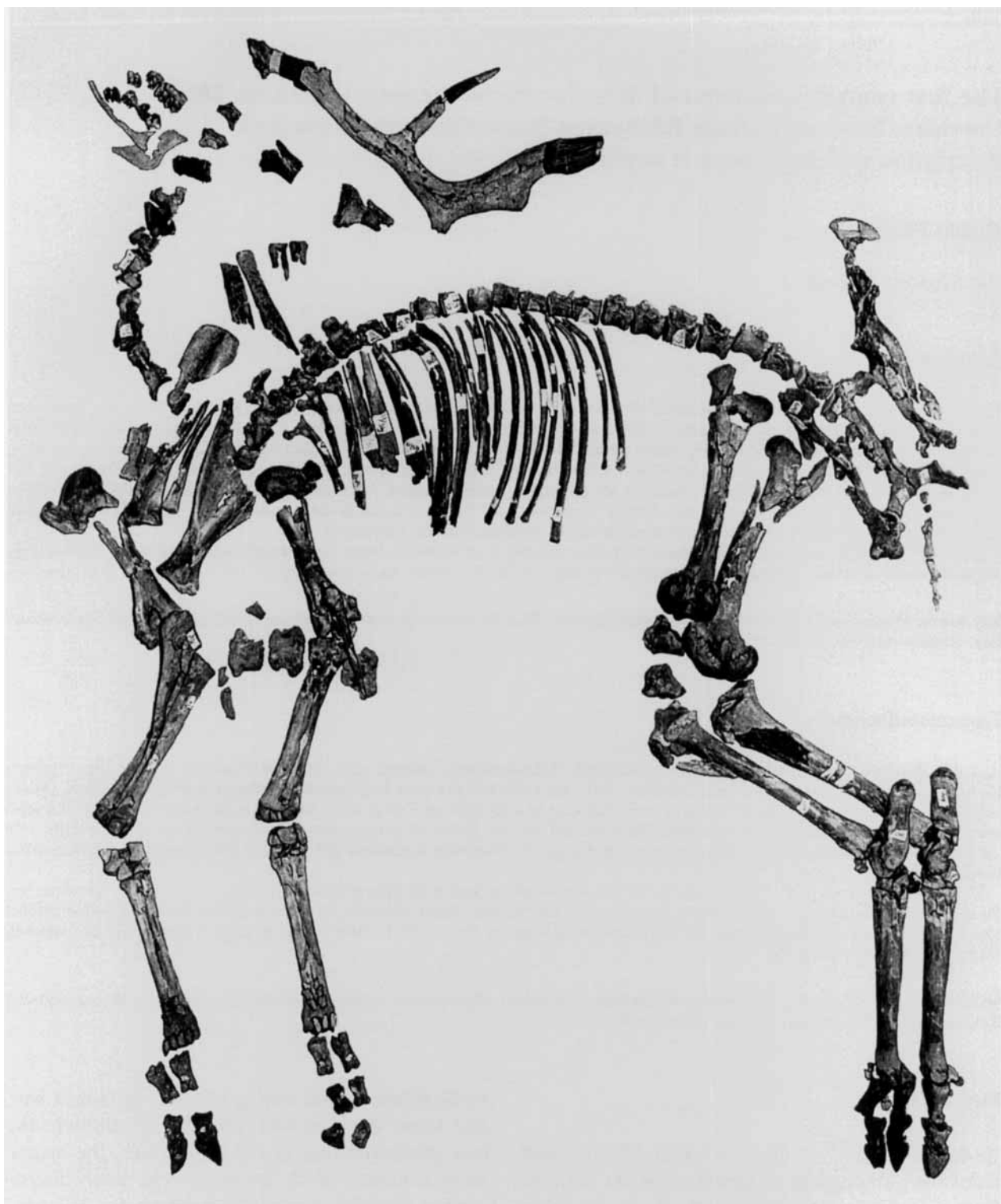


Fig. 1. The first articulated skeleton of a young male of *Megaloceros verticornis* (Dawkins, 1868) from Bilshausen.

(Meischner & Schneider 1967). Pollen analysis of the interglacial profile from Bilshausen was carried out by Müller (1965), and Grüger et al. (1994) who made detailed studies of the Middle Pleistocene warm phases of this area. Bittmann & Müller (1996) correlated the Kärlich Interglacial site with Bilshausen. The age of the

Brockentuff of Kärlich, 396,000 \pm 20,000 measured using the $^{40}\text{Ar}/^{39}\text{Ar}$ laser method by v. d. Bogaard et al. (1989) was fully compatible with the dating suggested by Bittmann & Müller (1996) on the basis of the vegetational development. The taphonomy of Bilshausen was interpreted by Meischner (1995) as follows: "Bils-

hausen was during its existence a meromictic pond ... fishes and mammals abound in the warved black shales. The skeleton of the giant deer showed no remnants of the skin, but the arrangement of the bones indicate that the corpse sank to the bottom, fell on the right side, and came to rest head-down on a slope. Bones maintained their original arrangement, but became disarticulated and were partly rotated, partly pulled-apart, by downslope movement of the still soft sediment." The skeleton of the young male deer of *Megaloceros verticornis* is especially important because it is the first articulated skeleton found for this species.

Fossil and recent cervids have been described primarily on the basis of antler-, skull- and tooth characters, and additionally on body size. Current morphological taxonomy splits the family Cervidae on the basis of a single character: absence (Hydropotinae) or presence (Odocoileinae + Cervinae) of antlers (Groves & Grubb 1987), even though the taxonomic value of antlers has been repeatedly questioned (see, for example, Scott & Janis 1993). Antlers show high variability within a species, and this is dependent on ontogenetic growth patterns and habitat conditions.

Unfortunately, previous workers attempted to ascertain relationships of cervids based only on the comparison of antler and skull characters. An example of this problem is the unresolved discussion concerning the relationships of the Recent fallow deer (*Dama dama*) and the giant deer (*Megaloceros giganteus*) which stems from the beginning of the last century. The presence of large, palmated antlers in *Dama dama* and *Megaloceros giganteus* suggested a close relationship between these two taxa (Freudenberg 1914, Geist 1971, 1987, Lister 1984). By contrast Thenius (1958) and Kahlke (1994) held the view that the giant deer must have evolved from deer with antlers that lacked any palmation. Investigations by Pfeiffer (1999a, in press) that also include postcranial characters, show that the genera *Megaloceros* and *Dama* belong to clearly separate lineages in the Pleistocene, and that their palmate antlers must have evolved independently.

The systematic position of *Megaloceros verticornis* has also been controversial (see below). On the basis of the skeleton from Bilshausen, and together with skulls, antlers, and selected postcranial skeletal material from adult individuals of *Megaloceros verticornis* from the Thuringian localities Süßenborn and Voigtstedt (Kahlke 1956, 1960, 1965, 1969) it is possible to determine the systematic position of this species

within the Pleistocene plesiometacarpal deer for the first time. Analysis of the morphology of the postcranial skeletal elements verifies a close relationship between *M. verticornis* and *M. giganteus*.

Gould (1974) showed that the dramatic size reduction of spike antlers in the advanced South American genera *Pudu* and *Mazama* suggests that the reversal of morphological trends is possible as a consequence of selection correlated with small body size. Some morphological characters seem therefore to be with highly homoplastic in ungulates (Scott & Janis 1993), and are difficult to use for determining phylogenetic relationships.

Material

The analysis conducted here was based on skeletons from males and females of a large number of Recent and fossil deer species, and the skeleton of *Megaloceros verticornis* from Bilshausen (Table 1). This taxon list includes the Recent telemetacarpal species *Alces alces*, *Rangifer tarandus*, *Capreolus capreolus*, *C. pygargus*, the Middle Pleistocene Roe deer *C. suessendorfensis*, the Lower Pleistocene plesiometacarpal species *Eucladoceros teguleensis*, *E. dicranios*, *Dama rhenana*, *Dama nestii*, the Middle Pleistocene *Megaloceros verticornis*, *M. giganteus*, *Cervus elaphus acronatus*, *Dama dama clactoniana*, *D. dama geisleriana*, and the extant forms *Cervus elaphus*, *C. nippon nippon*, *C. nippon hortulorum*, *Axis axis*, *D. dama mesopotamica*, and *D. dama dama*. Skeletons of the Recent *Moschus moschiferus* and skeletal material of the taxa *Blastomeryx* and *Parablastomeryx* from the Miocene of North America were added as outgroups.

In addition to skeletons, isolated bones of fossil taxa from different localities were also used. The scapula and pelvis, like the skull, were often broken. In the case of *Megaloceros verticornis*, the skeleton of the young stag from Bilshausen was analysed together with skulls, antlers and isolated postcranial bones of adult individuals from Süßenborn and Voigtstedt. Because the skull of the deer from Bilshausen is not preserved and this specimen represents a juvenile, it was necessary to study additional elements from adult individuals.

Method

A data matrix was coded for the 20 fossil and Recent deer listed above, and the antlerless musk deer, *Moschus moschiferus*, together with *Blastomeryx* and *Parablastomeryx* from the Miocene of North-America were used as outgroups. In current taxonomy, *Moschus* is commonly accepted as a close relative of the family Cervidae. *Blastomeryx* and *Parablastomeryx* share many ancestral features with early cervids including, for example, large upper canines.

The one-hundred and twenty-two morphological characters based on postcranial bones, antlers, skulls, and teeth are explained in Table 2, and listed in the data matrix (Table 3). The characters were coded as "unordered", and equally weighted, while missing data was denoted by a question mark. Polymorphic character states, which occur within a species with approximately the same frequency, were coded with the equate format $a = 0 + 2$; $b = 0 + 1$. Phylogenetic reconstructions were obtained by the maximum parsimony (MP)

method (PAUP 4.0, Swofford 1998), and the maximum-likelihood (ML) method (quartet puzzling approach: Strimmer & von Haeseler 1996). The robustness of the phylogeny was assessed using the following approaches: the bootstrap percentage (BT) (Felsenstein 1985) with 1000 resamplings, heuristic search mode; the Jackknife with 50% deletion, heuristic search mode, 1000 replicates; the reliability percentages (RP), i.e. the number of times the group appears after 10000 ML puzzling steps (Strimmer & von Haeseler 1996).

Taxonomy

Megaloceros verticornis (Dawkins, 1868)

Family **Cervidae** Goldfuß, 1820
Subfamily **Cervinae** Goldfuß, 1820
Genus **Megaloceros** Brookes, 1828

- 1862 *Megaceros Carnutorum* – Laugel, A.
- 1868 *Cervus verticornis* – Dawkins, B.
- 1869 *Cervus (euryceros) Belgrandi* – Belgrand, E.
- 1882 *Cervus dawkinsi* – Newton, E. T.
- 1886 *Cervus (Dama) priscus* – Moullade, E.
- 1889 *Cervus belgrandi* – Harmer, F.
- 1892 *Cervus pachygenis* – Pomel, A.
- 1903 *Cervus pliotarandoides* – de Alessandri, G.
- 1920 *Praemegaceros verticornis* – Portis, A.
- 1927 *Cervus megaceros mosbachensis* – Soergel, W.
- 1953 *Megaceros verticornis* – Azzaroli, A.
- 1953 'Cervus' obscurus – Azzaroli, A.
- 1956 *Orthogonoceros verticornis* – Kahlke, H.-D.
- 1956 *Dolichodoryceros süßenbornensis* – Kahlke, H.-D.
- 1992 *Megaceroides verticornis* – Azzaroli, A. & Mazza, P.
- 1993 *Megaloceros verticornis* – Lister, A.

The species *M. verticornis* was first described by Dawkins (1868), but initially referred to the genus *Cervus*.

Laugel (1862) described, with *Megaceros carnutorum* from St. Prest, the antler characters of *Megaloceros verticornis* (Pfeiffer 1999b), but figured teeth of *Alces*. Therefore, Heintz & Poplin (1981) used *carnutorum* for an alcine, *Alces carnutorum*. In any case the cervid material from St. Prest may belong to two or more species. Concerning *Praemegaceros*, Portis (1920) first used this genus name in connection with the species *carnutorum*. This cannot be regarded therefore as a valid foundation for *Praemegaceros*.

Kahlke (1956) referred *M. verticornis* to a new genus, *Orthogonoceros*, presumed here to be a junior synonym of *Megaloceros*.

Azzaroli & Mazza (1992) included *Megaloceros verticornis* in the genus *Megaceroides*, which was described by Joleaud (1914) on the basis of a giant deer from Algeria. The antlers of *M. algericus* (Lydekker 1890), the type species of *Megaceroides*, are poorly known, but the teeth of *M. algericus*, figured by Lydekker (1890) differ in their morphology from those of *M. verticornis*. Consequently, the systematic position of *M. algericus* within the giant deer has yet to be resolved.

Lister (1993, 1994) combined all giant deer species to a single genus *Megaloceros* following Azzaroli (1953). The name *Megaloceros* Brookes, 1828 (type species *M. giganteus*) has priority over *Megaceros* Owen 1842 (Lister 1987, International Commission on Zoological Nomenclature 1989), and the author follows this opinion here.

Description of the skeleton of *Megaloceros verticornis* from Bilshausen

Preservation

This young male individual of *M. verticornis* lay on its right side, legs parallel to one another (Fig. 1). The bones are dark brown, with well preserved surfaces, that usually permit detailed study of the morphological characters. The body is well preserved, but the cervical vertebral column is disarticulated, and the skull, the anterior cervical vertebrae, the main part of the left antler, parts of the lumbar vertebral column, and the sacrum are missing (Fig. 1). Some isolated lower and upper molars are preserved, important among which are the left upper M^3 and fragments of the lower m_3 . The last molars are completely developed, but show no (m_3) or only very little abrasion (M^3). At the age of 24 months the second dentition is complete in the extant genera *Cervus* (Habermehl 1961) and *Dama* (Rieck 1983). If *M. verticornis* developed the last lower and upper molars at the same ontogenetic stage, an age of two years is indicated for this stag at death. This observation is in accordance with several long bones that show incomplete fusion of their epiphyses. The juvenile age also explains the relatively small degree of antler development (Fig. 2) in comparison to adult individuals from Süßenborn (Kahlke 1956, 1969). The right antler is nearly complete, while the left antler is only presented by fragments of the first and second anterior tines.

Both humeri, femora, tibiae, and the metapodials were broken in their proximal part, but are reconstructed. The fragmentary pelvis, sacrum and coccygeal vertebrae were reconstructed, but yield no informative morphological details. All anterior and posterior phalanges are complete and well preserved. As the carpal and tarsal bones were fixed in position during the reconstruction of the skeleton neither measurements, nor morphological details could be collected for these elements.

Table 1
Skeletal material of the 20 cervid species studied in this investigation.

Recent:

<i>D. dama dama</i>	♂: 30	♀: 28
<i>D. dama mesopotamica</i>	♂: 12	♀: 12
<i>Axis axis</i>	♂: 8	♀: 10
<i>C. nippon nippon</i>	♂: 11	♀: 11
<i>C. nippon hortulorum</i>	♂: 6	♀: 6
<i>Cervus elaphus</i>	♂: 12	♀: 10
<i>Alces alces</i>	♂: 15	♀: 7
<i>Rangifer tarandus</i>	♂: 5	♀: 4
<i>Capreolus capreolus</i>	♂: 15	♀: 8–15
<i>Capreolus pygargus</i>	♂: 2	♀: 1

Archaeological sites:

<i>D. dama dama</i> (Kastanas, Demircihüyük)	♂/♀: 17
<i>D. dama mesopotamica</i> (Halawa, Kebara)	♂/♀: 6

Late Pleistocene:

<i>Dama dama</i> (Upper Rhine valley, Lehringen, Trafalgar Square)	♂/♀: 6	
<i>Megaloceros giganteus</i> (Upper Rhine valley, Schlutup, Ireland)	♂: 5–15	♀: 2–7
<i>Alces alces</i> (Upper Rhine, Valley, Magdeburg-Neustadt)	♂/♀: 7–11	

Middle Pleistocene

<i>D. dama geisalana</i> (Neumark-Nord)	♂: 47	♀: 15
<i>Cervus elaphus</i> (Neumark-Nord)	♂: 17	♀: 1
<i>D. dama clactoniana</i> (Clacton, Swanscombe, Jaywick, Grays, Riano, Valdemino, Melpignano)	♂/♀: 16–27	
<i>Cervus elaphus</i> (Clacton, Swanscombe, Jaywick, Grays)	♂/♀: 2–15	
<i>Cervus elaphus acoronatus</i> (Mosbach, Süßenborn, Voigtsdorf)	♂/♀: 8–23	
<i>Megaloceros verticornis</i> (Mosbach, Süßenborn, Voigtsdorf, Bilshausen)	♂/♀: 2–10	
<i>Capreolus suessenbornensis</i> (Mosbach, Süßenborn, Miesenheim)	♂/♀: 4–18	

Lower Pleistocene

<i>Dama nestii</i> (Tasso)	♂/♀: 12–29	
<i>Dama rhenana</i> (Senéze, Tegelen)	♂: 12–26	♀: 12–24
<i>Eucladoceros tegulensis</i> (Senéze, Tegelen)	♂/♀: 12–29	
<i>Eucladoceros dicranios</i> (Tasso)	♂/♀: 2–14	

The teeth and skeletal elements of *Megaloceros verticornis* from Bilshausen are relatively large and within the size range of those of *Megaloceros verticornis* from Süßenborn, and the giant deer, *M. giganteus*, from other Upper Pleistocene German localities (Table 4).

Antler

The antlers of *M. verticornis* always show a characteristic medially-curved tine at a point 4 to 8 centimetres above the burr, and this can be observed at the antler of the young stag from Bilshausen. In addition, some antlers of *M. verticornis* exhibits a growth near the base of the beam, ranging from a small bump to a strong tine, which is not developed on the antler from Bilshausen. Due to this variation some specimens with a long tine in this position have been separated as species by previous workers, such as *Cervus pliotarandoides* and '*Cervus obscurus*'.

Measures of the preserved right antler are given in Fig. 2. The height of the right pedicle

(HRst) is 55 mm, while its diameter (DRst), at 50.5 mm, is quite small. The burr is incomplete, with a preserved diameter (DR) of 56.5 mm, but must have been about 65 mm in life. These data support a juvenile age. The first anterior tine inserts at a right angle about 60 mm above the burr. The beam is rounded in its proximal part, with longitudinal ridges on its surface, but without pearls. It becomes flattened in the region where the second anterior tine branches off. A flattened posterior tine, now broken, also branched off 380 mm above the burr. The distal part of the beam shows a weakly developed palmation and is directed anteriorly. The distal part of the antler is missing, and the preserved length is 747 mm. The beam turns sideways and upwards above the burr.

Upper molars

From the right upper jaw a fragment with M^2 and M^3 is preserved, while from the left side, a fragment of M^1 , and the complete, isolated M^2

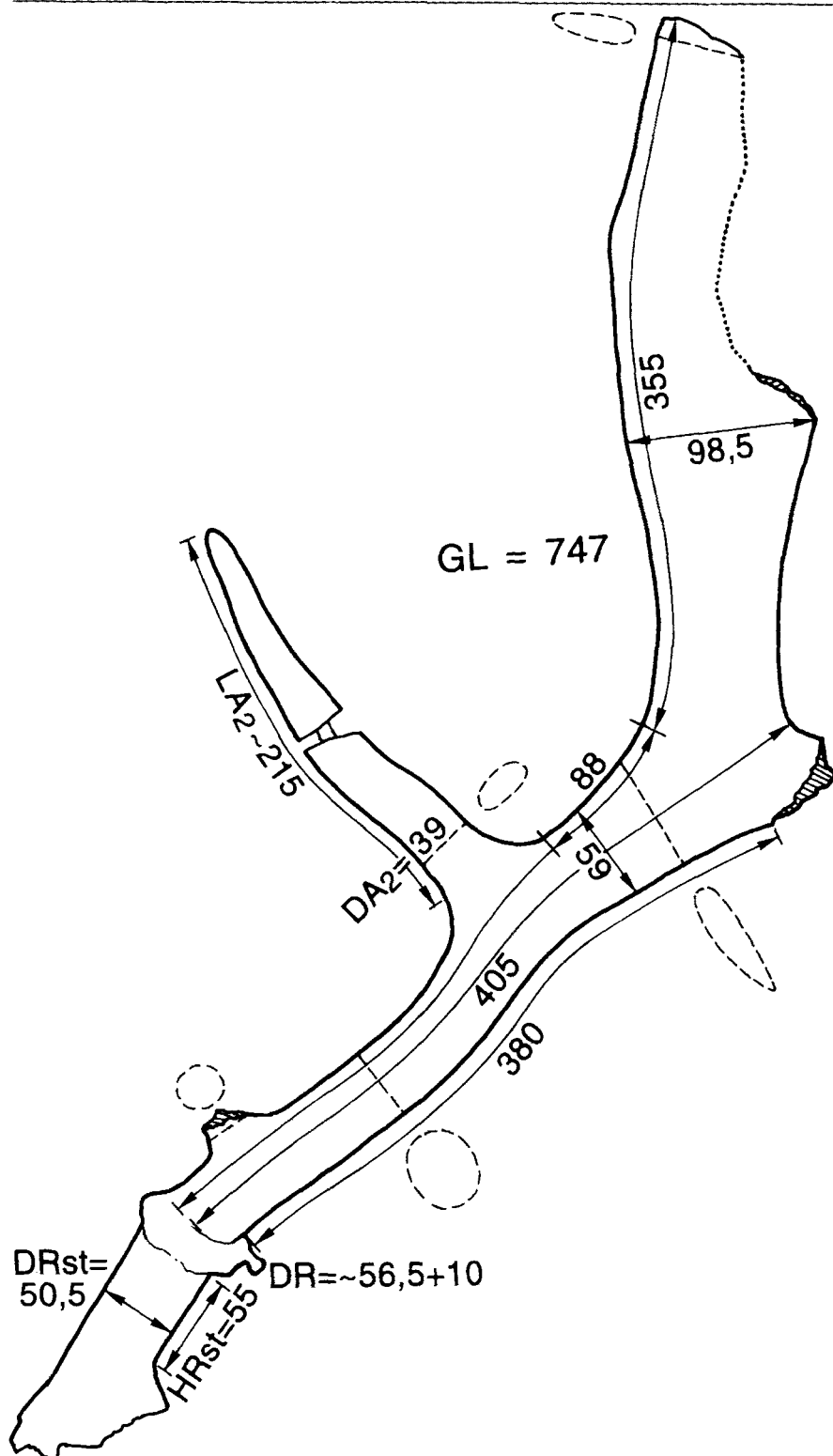


Fig. 2. Right antler of a two year old stag from Bilshausen indicating principal measurements (see explanation in the text). The development of the burr shows that the stag had shed an antler in the year before. The relatively small dimensions confirm a juvenile age.

and M^3 are measured (Table 4). All molars show well developed entostyli, a small anterior cingulum, and a well expressed posterior cingulum. The anterior and posterior lingual lobes bifurcate posteriorly (Fig. 3a).

Lower molars

A fragment of the left lower jaw is preserved, but lacks teeth. It is not pachognathous, as in

adult megalocerines, and only slightly thickened. The isolated lower right and left m_1 , and the left m_2 are preserved, the latter showing little abrasion. An anterior cingulum is well developed, and the ectostyliid is small (Fig. 3b). Fragments of the lower right and left m_3 show no abrasion. This indicates that the individual is of about two years in age.

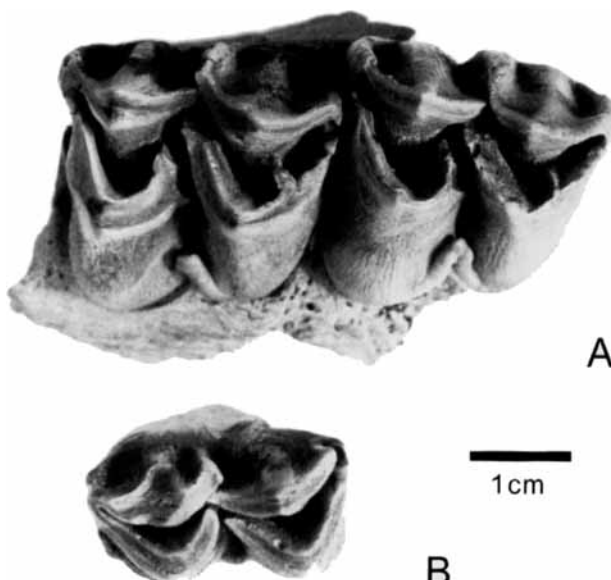


Fig. 3. A. Left upper molars (M^2 , M^3) in occlusal view. M^3 shows little abrasion, indicating an individual age of two years at the time of death. All molars show well developed entostyli, a small anterior cingulum, and a well expressed posterior cingulum. The anterior and posterior lingual lobes are bifurcated posteriorly. B. Right lower molar (m_1) in occlusal view. An anterior cingulum is well developed, the ectostyloid is small.

Vertebral column

Axis: Only the cranial facet of the axis could be measured, its widths is 108.5 mm (BFcr, v. d. Driesch 1976), and the distal epiphysis is not fused.

Only the corpi of the 3rd–7th cervical vertebrae are preserved. Each epiphysis is separated from the corpus. Corpus lengths are in the size range typical for *Megaloceros*. The shape of the cranial epiphyses is similar to those of *Megaloceros giganteus*, flattened or concave dorsally, wide, and rounded, a diagnostic character for *Megaloceros*.

The corpus of each thoracic vertebrae is preserved, but not one of the epiphyses is fused. By contrast, the proximal epiphysis of the first lumbar vertebra is fused and shows a weakly depressed margin laterally.

Scapula

The cavitas glenoidalis is round and wider than long (cha. 12 in the description of character states, Table 2) and it has no V-shaped cavity in its articular surface (cha. 13). the tuberculum supraglenoidale is short, coarse, and not medially curved (cha. 14) as in *Megaloceros giganteus*. *M. verticornis* has no foramen dorsally between the processus coracoideus and the cavitas glenoidalis (cha. 15) as in most species of deer, while *M.*

giganteus has a large foramen in this position. The scapula shaft is robust, but not especially widened as in adult individuals of *M. giganteus* (cha. 17). This character is strongly influenced by antler development. Consequently, the relatively juvenile age and the small antler of the individual from Bilshausen reflect the weaker expression of this feature.

Humerus

The proximal epiphyses of both humeri are not fused, but the distal epiphyses were just beginning to fuse to the diaphysis at the time of death. Only characters of the distal part could be determined. The fossa radialis shows two rounded scores (cha. 21), a character that is diagnostic for *M. verticornis* and *M. giganteus*. The morphology is generally similar to that of *Megaloceros giganteus*, except that the epicondylus lateralis has no pronounced bony knob (cha. 22).

Radius and Ulna

The caput olecrani is not fused to the ulna diaphysis, and the fusion of the distal epiphysis of the radius is incomplete. In addition, there is no bony connection between the diaphyses of the radius and ulna. This is consistent with an ontogenetic stage of two years. The attachment of the ligamentum collaterale laterale at the proximal end of the radius diaphysis projects out laterally, and slopes a little downwards (cha. 26). *Megaloceros verticornis* from Bilshausen shares this development with *Megaloceros giganteus* and the genus *Cervus*. Characters 34–37 could not be unequivocally assessed because the stag was relatively young.

Metacarpus III + IV

The epiphyses of the right and left metacarpus III + IV are nearly completely fused. In most species of deer this epiphysis fuses in the end of the second year. The dimensions of these bones are similar to those of *Megaloceros giganteus*, moreover the specimen of *M. verticornis* from Bilshausen has also stout diaphyses of MC III + IV as is typical for the giant deer. The morphology of the distal end of MC III + IV is generally similar to that of *Megaloceros verticornis* (cha. 43, 44, 45) and to most plesiometacarpal species of deer.

Pelvis

The bones of the pelvis are broken into numerous pieces, and no metric data could be obtained. The symphysis pelvina was not fused at the time of death.

Table 2
Description of 122 skeletal characters and their character states for various cervids used for the computer-aided phylogeny reconstruction.

Σ	skeletal element	Code	Description of character states	Σ	skeletal element	Code	Description of character states
1	Atlas	0	Alae straight	13	Scapula	0	the cav. glenoidalis shows no V-shaped cavity in its articular surface
		1	Alae convex			1	the cav. glenoidalis shows a V-shaped cavity in a few cases
		2	Alae concave			2	the cav. glenoidalis shows a V-shaped cavity with a frequency up to 25%
2	Atlas	0	Atlas cranially and caudally narrow			3	the cav. glenoidalis shows a V-shaped cavity with a frequency up to 50%
		1	Atlas cranially narrow, caudally broad			4	the cav. glenoidalis shows a V-shaped cavity with a frequency up to 85%
		2	Alae cranially and caudally broad				
3	Atlas	0	Alae not elongated caudally	14	Scapula	0	the tuberculum supraglenoidale is slender, medially curved
		1	Alae a little elongated caudally			1	the tub. sup. is strong, elongated, medially curved
		2	Alae especially elongated caudally			2	the tub. sup. is especially long
		3	Alae especially elongated and widened caudally			3	the tub. sup. is especially strong, long, not ventrally curved
4	Axis	0	Spina dorsalis low, straight, cranially pointed	15	Scapula	0	the tub. sup. is short, coarse, not ventrally curved
		1	S.d. cranially rounded, caudally rising			1	no foramen dorsally between proc. coracoideus and cav. glenoidalis
		2	S.d. cranially pointed, caudally rising			2	a large foramen dorsally between proc. cor. and cav. Glenoidalis
		3	S.d. cranially rounded, caudally extremely rising				
5	Axis	0	Dens short	16	Scapula	0	the spine scapulae ends proximally with a peak, forming an angle of 80-90° with the shaft
		1	Dens elongated			1	the spine scapulae is especially elongated in the direction of the cav. glenoidalis
6	Axis	0	S.d. inserts above the dens in lateral view	17	Scapula	0	the spine scapulae ends proximally with an angle of about 100° with the shaft
		1	S. d. inserts behind the dens in lateral view			2	the spine shaft is slender
						1	the spine shaft is strong
						2	the spine shaft is especially widened
7	cervical-vertebrae	0	proximal epiphysis varies in its shape	18	Humerus	0	the tuberculum majus is flattend, with no cavity
		1	prox. epiphysis heart-shaped, dorsally rounded			1	the tub. majus is slightly indented in a few cases
		2	prox. epiphysis angular			2	the tub. majus is indented in most cases
		3	prox. epiphysis rounded, wide, dorsally concave			3	the tub. majus is deeply indented
8	cervical-vertebrae	0	no tubercle on the caudal process	19	Humerus	0	the tub. majus without visible muscle attachment laterally
		1	a tubercle on the caudal process			1	the tub. majus with a weak muscle attachment laterally
9	cervical-vertebrae	0	transverse processes short, narrow			2	the tub. majus with a marked muscle attachment laterally
		1	transverse processes short, broad				
		2	transverse processes elongated, narrow				
10	6th lumbar vertebra	0	distal epiphysis without any process	20	Humerus	0	the epicondylus humeri is axially stronger than laterally
		1	distal epiphysis with short processes laterally			1	the epicondylus humeri is axially also slender in a few cases
		2	distal epiphysis with elongated processes laterally			2	the epicondylus humeri is axially slender with a frequency up to 50%
		3	distal epiphysis with short processes ventral, laterally directed			3	the epicondylus humeri is axially slender in most cases
11	6th lumbar vertebra	0	Os sacrum and 6th lumb. vertebra with a flexible connection			4	the epicondylus humeri is axially especially strong in a few cases
		1	Os sacrum and 6th lumb. vertebra are interlocked			5	the epicondylus humeri is axially always especially strong
12	Scapula	0	the cav. glenoidalis is oval, more elongated than wide	21	Humerus	0	the scores of the fossa radialis show variable shapes
		1	the cav. glenoidalis shows a knob in direction to the spine in a few cases			1	the fossa. radialis has two wedge-shaped scores
		2	the knob occurs with a frequency of 25% - 50%			2	the lateral score of the fossa radialis is lacking in a few cases
		3	the knob occurs with a frequency of more than 50%			3	the lateral score of the fossa radialis is lacking with a frequency up to 50%
		4	the cav. glenoidalis shows a knob in direction of the tub. supraglenoidale in a few cases			4	the fossa radialis shows laterally no score
		5	the cav. glenoidalis is wider than long			5	the fossa radialis shows two rounded scores

$\frac{1}{2}$	skeletal element	Code	Description of character states	$\frac{1}{2}$	skeletal element	Code	Description of character states
22	Humerus	0	epicondylus lateralis with a knob varying in size	32	Radius	0	the axial carpal facet forms no dorsally directed triangle
		1	epic. lateralis with a strong knob			1	the axial carpal facet forms a dorsally directed triangle
		2	epic. lateralis without a knob	33	Radius	0	the diaphysis has axially, 1 cm posteriorly of the cranial facet no depression
		3	epic. lateralis with a groove			1	the diaphysis is axially deepend, 1 cm posteriorly of the cranial facet
23	Humerus	0	margin of the fossa olecrani with a variable shape	34	Radius	0	the diaphysis has axially no keel
		1	margin of the fossa olecrani wavy, horizontally directed			1	the diaphysis is axially keeled
		2	margin of the fossa olecrani straight, horizontally	35	Ulna	0	the edge of the tuber olecrani is rounded with a V-shaped score
		3	margin of the fossa radialis turns downwards laterally			1	the edge of the tuber olecrani is rounded with a weak depression
24	Humerus	0	the fossa olecrani is evenly deep	36	Ulna	0	the lateral side of the olecranon shows a rounded muscle attachment in most cases
		1	the fossa olecrani is axially deeper			1	the lateral side of the olecranon always shows a rounded muscle attachment
		2	the fossa olecrani is axially especially deep			2	the muscle attachment forms a ridge
25	Humerus	0	Diaphysis laterally rounded in its distal part			3	no muscle attachment is visible on the lateral side of the olecranon
		1	Diaphysis laterally keeled	37	Ulna+Radius	0	the suture between radius and ulna shows no elongated foramen
26	Radius	0	the attachment of the lig. col. laterale sticks out laterally, sloping a little downwards			1	the suture between radius and ulna shows an elongated foramen in its posterior part
		1	the att. of the lig. col. lat. sticks out lat., rising clearly above the cran. fac. in a few cases	38	MC III+IV	0	sidemetapodials reduced distally (plesiometacarpal)
		2	character state 1 with a frequency up to 50%			1	side metapodials reduced proximally (telometacarpal)
		3	character state 1 with a frequency of more than 50%	39	MC III + IV	0	the scutus longitudinalis is always deep
		4	the att. of the lig. col. lat. sticks out laterally, almost rising clearly above the cran. facet			1	the scutus longitudinalis is deep in most cases
		X	the att. of the lig. col. lat. slopes straight downwards			2	the scutus longitudinalis is visible as a score or connated with the same frequency
						3	the scutus longitudinalis is connated
27	Radius	0	the attachment of the lig. col. med. is rough, elongated, facing up to the cran. facet	40	MC III + IV	0	the proximal basis is not connated posteriorly
		1	the att. of the lig. col. med. is oval, facing 1 cm below the cran. f. in a few cases			1	the proximal basis is not connated posteriorly in most cases
		2	the att. of the lig. col. med. is oval, facing 1 cm below the cran. f. in most cases			2	the proximal basis is connated posteriorly in half of the cases
		3	the att. of the lig. col. med. is oval, almost facing 1 cm below the cranial facet			3	the proximal basis is connated posteriorly in most cases
28	Radius	0	the shape of the margo lateralis is variable			4	the proximal basis is connated posteriorly
		1	the margo lat. forms a distant lip in most cases				
		2	the margo lat. always forms a distant lip				
		3	the margo lateralis is planar, bending off posteriorly to the diaphysis	41	MC III + IV	0	the proximal facet of MC III projects equally or beyond the f. of MC IV in post. view
		4	the cranial facet shows rough breaks in its surface with the shape of (a), (b), and (c)			1	the prox. f. of MC III projects clearly beyond the f. of MC IV in post. view
		5	the cran. f. shows a rough, laterally directed break in its surface (a)			2	the MC III and IV project approximately equally with their proximal facets
		6	the cran. f. shows two circular breaks in st surface (b)	42	MC III + IV	0	the dorsal edge of the cranial facet is rounded
		7	the cran. f. shows one central break, extending to the post. margin (c) together with (b)			1	the dorsal edge of the cranial facet is rounded or laterally broadened
		8	the cran. f. shows always one central break, extending to the posterior margin (c)			2	the dorsal edge of the cranial facet looks more triangular in most cases
		9	the cran. f. shows rough breaks in its surface with the shape of (a) and (c)			3	the dorsal edge of the cranial facet looks more triangular
		10	the cran. f. shows a deep anterior posteriorly directed groove			4	the dorsal edge of the cranial facet looks triangular, laterally broadened
30	Radius	0	the cranial facet shows no foramen in the deep anterior posteriorly directed groove	43	MC III + IV	0	the dorsal edge of the cranial facet is laterally especially broadened
		1	the cran. f. shows a deep foramen in the deep anterior posteriorly directed groove			5	the distal trochlea is separated dorsally by pits from the diaphysis
31	Radius	0	the carpal facets are dorsally equal in height			1	pits are missing
		1	the carpal facet is axial higher than lateral				

Σ	skeletal element	Σ	Description of character states	Σ	skeletal element	Σ	Description of character states
44	MC III + IV distal	0	the gap between the distal trocheae of MC III and IV forms a key hole	55	Tibia proximal	0	the tuberosity for the ligamentum cruciatum forms an elongated U-shape
	1	the gap between the distal trocheae of MC III and IV has parallel margins			1	the tub. for the lig. cruc. forms an elongated or short U-shape	
45	MC III + IV distal	0	the diaphysis shows long, weakly expressed keels posteriorly		2	the tub. for the lig. cruc. is short, forming a weak U-shape	
	1	the diaphysis has a flattened surface posteriorly			3	the tub. for the lig. cruc. shows a depression laterally	
46	Femur proximal	0	the fossa trochanterica shows a weak, U-shaped depression in its margin	56	Tibia distal	0	the tub. for the lig. col. tars. mediales is horizontal, forming a pronounced point anteriorly
	1	in most cases the f. trochanterica shows a deep U-shaped depression in its margin			1	the att. of the lig. col. tars. mediales is horizontally directed, ending anteriorly	
	2	the f. trochanterica shows always a deep U-shaped depression in its margin			2	the att. of the lig. col. tars. mediales turns upwards, forming a curve	
	3	the f. trochanterica shows a flat, diagonally directed margin			3	the att. of the lig. col. tars. mediales is roundish, not clear cut	
47	Femur proximal	0	the edge of the trochanter major forms a flat-topped shape	57	Tibia distal	0	the dorsal facet in contact with the malleolus lateralis is small
	1	the edge of the t. major is rising anteriorly in a few cases			1	the dors. fac. in contact with the mal. lateralis is variable in size	
	2	the edge of the t. major is rising anteriorly			2	the dors. f. in contact with the mal. lateralis is very small	
	3	the edge of the t. major shows two small scores			3	the dors. f. in contact with the mal. lateralis is enlarged	
	4	the edge of the t. major has one deep score in the middle			4	the dors. f. in contact with the mal. lateralis is enlarged and pronounced	
48	Femur proximal	0	the muscle attachment laterally at the trochanter major forms a weak keel.	58	Tibia distal	0	the lateral part of the coxale tibiae shows a small, pronounced point
	1	the muscle att. laterally at the t. major forms a weak keel or a knob.			1	the pronounced point is enlarged in some cases	
	2	the m. att. laterally at the t. major forms a knob.			2	the point at the coxale tibiae is always enlarged and very pronounced	
	3	the m. att. laterally at the t. major forms a rough, depressed score			3	the lateral part of the coxale tibiae is nearly flattened, forming a weak curve	
	4	the m. att. laterally at the t. major forms a marked keel.			4		
49	Femur proximal	0	the att. of the m. vastus intermedius forms a weak knob at the proximal femur	59	MT III+IV proximal	0	the MT III and IV project approximately equally with their proximal facets
	1	the knob is accompanied by a depression in some cases			1	the proximal facet of MT III projects clearly above the facet of MT IV	
	2	the knob is usually accompanied by a depression			0	on the axial edge between MT III and MT II a bulge exceeds the proximal facets	
	3	the att. of the m. vast. interm. forms an elongated keel			1	the bulge is especially pronounced in most cases	
	4	the att. of the m. vast. interm. forms a marked knob distally of the troch. major			2	the bulge is always very pronounced	
50	Femur	0	the diaphysis is rounded in cross section			3	the bulge between the facets of MT III and MT II is accompanied by a small gully
	1	the diaphysis is posteriorly keeled in cross section			4	the bulge is very small, accompanied by a gully	
51	Femur distal	0	the facies poplitea is flattened, rough			5	on the axial edge between MT III and MT II exists only a gully
	1	the f. poplitea forms a rough, prominent tuberosity			6	the proximal facets of MT III and MT II border on each other, there is no bulge or gully	
52	Femur distal	0	the fossa intercondylaris is shallow, the distance of the condyles is small	61	MT III + IV proximal	0	the shape of the posterior facet in contact with the cubo-navicular bone is short
	1	the f. intercond. varies in its depth, the distance of the condyles is wide			1	the post. f. is more elongated, overlapping with the facet of the MT III	
	2	the f. intercond. is deep, the distance of the condyles is small			2	the post. f. is more elongated, overlapping up to the middle of the facet of the MT III	
53	Tibia proximal	0	the internal peak of the tub. intercondylare projects clearly beyond the external peak			3	the post. f. is elongated, exceeding the middle of the facet of the MT III
	1	the tub. intercond. projects approximately equally with its internal and external peak			4	the post. f. is especially elongated, transversally directed, flattened	
	2	the tub. intercond. projects approximately equally with its internal and external peak			0	the posterior facet projects slightly above the facets of MT III and MT IV	
54	Tibia proximal	0	the area intercond. centralis is post. short, restricted by the tub. for the lig. cruciatum			1	the post. f. is short, and forms a pronounced peak in the middle between MT III and IV
	1	the a. i. c. is laterally elongated, the facet of the lateral condyle is weakly elongated			2	the post. f. is elongated, with a small peak in the middle between MT III and IV	
	2	the a. i. c. forms a gully, the facet of the lat. condyle is distinctly elongated posteriorly			3	the post. f. is elongated and projects clearly above the facets of MT III and IV	
					4	the post. f. is flattened, projecting equally with the facets of MT III and IV	

σ_2	skeletal element	Code	Description of character states	σ_2	skeletal element	σ_2	Description of character states
63	MT III + IV proximal	0 1	one small, posteriorly elongated foramen is located betw. the facets of MT III and IV the foramen can have a small or wider opening	73	Talus post. view	0 1	lat. a weak groove borders the dist. part of the troch. in contact with the cubonavic. proc. the groove is more steeply inclined, forming an exactly adjusted connection with the c. p.
		2	the foramen has a wide, posteriorly elongated opening	74	Talus ant. view	0 1	small bulge laterally between the trochlea talis prox. and dist. in anterior view pronounced bulge laterally between the trochlea talis prox. and dist. in anterior view
		3	the canalis metatarsi can end in one small foramen or in two small foramina	75	1st Ph. ant. post. view	0 1	proximal two elongated bulges axially and laterally exceed the middle of the diaphysis the lateral bulge is shorter in most cases
		4	the canalis metatarsi can end in one wider foramen and a network of pores			2	the axial bulge is always much longer than the lateral one
		5	the canalis metatarsi ends always in two foramina			3	the expression of the bulges varies between 0, 1, and 4
64	MT III + IV distal ordered	0 1 2 3	at the distal end of the diaph. a small split persists between MT III + IV in adult individ. at the dist. end of the diaph. a small split persists between MT III + IV in most cases at the dist. end of the diaph. a small split persists between MT III + IV in a few cases the distal end of the diaphysis shows no split			4	the axial, very pronounced bulge reaches the middle of the diaph., a lat. bulge is lacking
		65	MT III+IV	0 1	the diaphysis is posterior or weakly keeled the diaphysis has posterior two pronounced keels	5	the expression of the bulges varies between 0, 7
		66	MT III+IV	0 1 2 3 4	the diaphysis has a medium diameter the diaphysis is slender the diaphysis is very slender the diaphysis is strong the diaphysis is very strong	6	expression 0 is rare, expression 7 occurs in most cases
		67	Calcaneus	0 1 2 3 4	small step between the edge of the sust. tali and the art. facet of the calc. shaft the step is usually small; but pronounced in a few cases the step is pronounced in most cases the step is clearly pronounced the edge of the sust. tali merges without any step to the margin of art. surface	77	the proximal bulges are strong but short, never reaching the middle of the diaphysis
		68	Calcaneus	0 1	the shaft of the calcaneus is slender the shaft is strong	78	the cross section of the diaphysis is somewhat smaller than the prox. epiphysis
		69	Calcaneus	0 1	the proc. coracoideus is small the proc. coracoideus forms a pronounced peak		1 the diaphysis is slender, but can be stronger in adult stages
		70	Talus corpus	0 1 2 3	the dist. part of the wave-like facet in contact with the talus is especially small the lateral extension of the ridge at the corpus tali varies in its proximal and distal part the lat. ext. of the ridge at the c. tali is equal in its proximal and distal part the lat. ext. of the ridge is greater in its proximal part than in its distal part	79	2 the diaphysis is always slender
		71	Talus capitum	0 1 2 3 4	the lat. ridge at the c. tali is pronounced in its proximal part and ends in the distal part trochlea talis distalis without a V-shaped pit a V-shaped pit in the tr. talis dist. occurs in a few cases a V-shaped pit occurs with a frequency of about 50% a V-shaped pit occurs in most cases trochlea talis distalis with a flat U-shaped pit	80	3 the diaphysis is very slender and elongated
		72	Talus posterior view	0 1 2 3	trochlea talis distalis with a deep, vertical pit a pit in the trochlea talis distalis is lacking trochlea talis distalis with a transversally directed pit trochlea talis distalis with a small depression axially	81	4 the diaphysis is especially strong
						5 a U-shaped score is always lacking in the proximal facet	the 1st phalanx post. shows two short, weakly expressed bulges anteriorly
						6 the margin of the distal trochlea shows a weak V-shape	0 The 1st phalanx post. shows two short, weakly expressed bulges anteriorly
						7 the margin of the distal trochlea shows a weak waveline	1 the axial bulge is elongated and more pronounced together with (0)
						8 the margin of the distal trochlea is flat	2 together with character state (0) occurs (3)
						9 the margin of the dist. tr. is wavy, ending in an elongated peak axially	3 the axial bulge is weak but rough, reaching the middle of the diaphysis
						10 the tendon attachment lateral. on the middle of the diaphysis varies in its expression	0 the tendon attachment lateral. on the middle of the diaphysis varies in its expression
						11 the tend. att. on the mid. of the diaph. is expressed as a tuberosity in most cases	1 the tend. att. on the mid. of the diaph. is expressed as a tuberosity in most cases
						12 character state (1) is always developed	2 character state (1) is always developed
						13 the tend. att. is expressed only by a rough surface	3 the tend. att. is expressed only by a rough surface
						14 the lat. tend. att. on the diaphysis is located very distally	4 the lat. tend. att. on the diaphysis is located very distally
						15 two marked tuberosities axially and laterally are located on the middle of the diaphysis	5 two marked tuberosities axially and laterally are located on the middle of the diaphysis
						16 the margin of the distal trochlea is weakly V-shaped	0 the margin of the distal trochlea is weakly V-shaped
						17 the margin of the distal talis shows (0) and (3) with an equal frequency	1 the margin of the distal talis shows (0) and (3) with an equal frequency
						18 character state (3) occurs with a higher frequency than (0)	2 character state (3) occurs with a higher frequency than (0)

$\frac{9}{2}$	skeletal element	Description of character states	$\frac{9}{2}$	skeletal element	Description of character states
81	3	the margin of the distal trochlea forms a weak waveline	93	browtine	0 a browtine (A1) is lacking
	4	the margin of the distal trochlea shows (0) and (5) with equal frequency		A1	1 the browtine inserts high above the burr, forming an acute angle with the beam 2 the browtine inserts 4 cm above the burr, at right angles to the beam 3 the browtine inserts directly above the burr, forming an obtuse angle with the beam
	5	the margin of the distal trochlea is flattened			4 the browtine is flattened, with furcated ends
	6	the margin of the distal trochlea is flattened, but wavy in a few cases			5 the browtine is almost reduced
82	1st Ph. post. post. view	0 the sagittally directed score in the distal trochlea is always symmetrical 1 the s. directed sc. in the dist. t. is symm. or asymm. with an equal frequency	94	second ant. tine (A2)	0 a second anterior tine (A2) is lacking 1 the A2 inserts directly above the A1
	2	the sagittally directed score in the distal trochlea is always asymmetrical			2 the A2 inserts clearly above the A1
83	1st Ph. post. ant. view	0 the lateral edge of the 1st pha. post. is slightly bent inwards in most cases 1 the lateral edge of the 1st pha. post. is slightly bent inwards	95	A2	0 a second anterior tine (A2) is lacking 1 the A2 is weaker than the A1 2 the A2 is stronger than the A1
	2	2 the lateral edge of the 1st pha. post. is straight, not bent inwards			2 the A2 is weaker than the A1
84	1st Ph. post. ant. view	0 the diaphysis is strong 1 the diaphysis is slender	96	A3	0 a third anterior tine (A3) is lacking 1 A3 is developed
	2	2 the diaphysis is very slender, axially curved inward			0 posterior tines are lacking 1 posterior tines are rare, rounded in cross section 2 posterior tines are long, flattened 3 posterior tines are numerous but very short 4 posterior tines are almost reduced
85	2nd Ph. ant. post. view	0 the prox. att. of tendons are expressed as bulges lat. and ax., exceeding the prox. facet 1 the axial bulge is especially elevated in most cases	97	posterior tines	0 the antlers show no palmation 1 the palmation is restricted to the terminal fork 2 the beam and the tines are palmated 3 a rounded beam merges to a strongly developed palm
	2	2 the axial bulge is almost especially elevated			4 the antlers show no palmation
	3	3 the axial bulge is especially elevated			1 the beam ends with a simple bifurcation
86	2nd Ph. ant. post. view	0 the distal trochlea forms an elongated peak axially 1 the distal trochlea forms an elongated peak axially in most cases	98	palmation	2 terminal tines solely orientated anteriorly
	2	2 the distal trochlea shows two short peaks axially and laterally			3 terminal tines orientated anteriorly in most cases
	3	3 the distal trochlea shows a weakly expressed peak axially			4 terminal tines well balanced orientated anteriorly and posteriorly
87	2nd Ph. ant. post. view	0 the distal trochlea is axially a little broader than laterally 1 the distal trochlea is axially clearly broader than laterally	99	direction of terminal tines	5 terminal tines orientated posteriorly in most cases
	2	0 the proximal diaphysis shows no pit laterally 1 the proximal diaphysis shows a pit laterally			6 terminal tines solely orientated posteriorly
88	2nd Ph. ant. ant. view	0 the proximal diaphysis shows no pit laterally 1 the proximal diaphysis shows a pit laterally	100	bifurcation of tines	0 bifurcated tines are lacking 1 bifurcated tines are rare 2 bifurcated tines are frequent
89	3rd Phal. bottom side	0 the sole of the 3rd phalanx is axially edged 1 the sole of the 3rd phalanx is bent inwards axially, not edged in several cases			0 beam short, rounded 1 beam elongated, rounded 2 beam elongated, flattened
90	3rd Phal. post. view	0 lat. part of the fac. in contact with the 2nd phal. as broad as the axial part of the fac., elongated prox. 1 lat. part of the f. in contact with the 2nd pha. is narrow, but very elongated prox., girding the ax. part of the f. prox.			3 beam extremely long, rounded, merging into a palm 4 beam long, rounded, merging into a palm 5 beam extremely short, merging into a palm
91	3rd Phal. lat. view	0 3rd phalanx with a triangular shape in lateral view 1 3rd phalanx dorsally arched, rounded			x no beam
92	antler	0 the beam forms a simple peak 1 the beam ends with a bifurcation	101	beam	
	2	2 three-point antler			
	3	3 four-point antler			
	4	4 five-point antler			
	5	5 six points or more			
	6	6 palmated antler			
	7	7 totally different construction			
	x	x no beam			

Σ_2	skeletal element	Code	Description of character states	Σ_2	skeletal element	Σ_2	Description of character states
102	beam surface	0 1 2 3	a pearly surface to the beam is lacking a pearly surface is weakly expressed a pearly surface is strongly expressed a pearly surface is most extensively expressed	110	ethmoid vacuity	0 1 2	ethmoid vacuity large, elongated ethmoid vacuity small ethmoid vacuity nearly connated
103	beam position	0 1 2 3 4 5 x	the beams are directed upright, nearly parallel slided the beams slope a little transversally the beams bend transversally, posteriorly and are curved upright the beam is curved horizontally, the antler is broadened transversally the beam inserts transversally at the skull, the antler is transversally directed no beam	111	skull sutures	0 1	sturures of the skull are almost visible in adult individuals
104	beam length	0 1 2 3 4 5 6 x	the beams are very short, less than 30 cm length of the beam 30 - 80 cm length of the beam up to 100 cm length of the beam up to 150 cm, lofty length of the beam up to 200 cm, lofty length of the beam up to 250 cm, transversally directed length of the beam up to 400 cm, transversally directed no beam	112	upper premolars	0 1	no cingulum occurs on the upper P4. a weak cingulum occurs in the upper P4.
105	pedicile	0 1 2 x	pedicile very long, circular in cross-section pedicile short, circular in cross-section pedicile very short, anterior-posteriorly elongated in cross-section no pedicile	113	upper premolars	0 1	anterior, lingual wing of the premolars without folds inside, or with one simple fold anterior, lingual wing of the premolars with a reticulated fold inside
106	frontal bone	0 1	frontal bone not thickened between the pediciles frontal bone thickened and arched between the pediciles	114	upper molars	0 1 2	entostyli are strongly developed entostyli are small, not always abundant entostyli are lacking
107	linea nucha	0 1 2 3 4	expressed as simple, rounded crest nuchal crest laterally strengthened, and broadened nuchal crest forms a S-shape nuchal crest forms a double-S-shape nuchal crest is angular in the middle	115	upper check-teeth	0 1	upper molars show tabially an equal, uniform row. the row of the up. teeth has a step-like outline labially, shifted from ant. to post.
108	occipital bone	0 1 2	the height of the occipital bone between the nuchal crest and the condyles is low the occipital part is high the occipital part is high, the nuchal crest projects clearly behind the condyles	116	upper upper molars	0 1 2 3	folds inside the anterior wing of the protocone are lacking simple folds inside the ant. wing of the protocone are clearly developed furcated folds inside the ant. wing of the protocone form an island inside (Alces) folds inside the ant. wing reticulated (<i>Rangifer</i>)
109	lacrimal orifices	0 1	two lacrimal orifices one lacrimal orifice	117	upper canine	0 1 2	an upper canine is strongly developed in ♂ an upper canine is rudimentarily developed in ♂ an upper canine is always lacking
110				118	upper M3	0	crown of the upper M3 posteriorly deeply notched
111				119	mandible P3	0 1 2	crown of the upper M3 posteriorly connated P3 not molarised P3 with a post-metacristid
112				120	mandible P4	0 1 2 3 4	postento- and hypocristid are connated P4 not molarised a praemetacristid is developed entocristid and metacristid wings fused, forming a diagonal crest (Alces, <i>Rangifer</i>) P4 almost molarised P4 always molarised
113				121	mandible M3	0 1 2	the last lobe of the M3 is very small the last lobe of M3 is strongly developed, posteriorly rounded the last lobe is strongly developed, with a pointed end posteriorly in a few cases.
114				122	mandible	0 1 2	the mandible is narrow in cross-section, not thickened the mandible is a little thickend in cross-section, (weakly pachyglossous) the mandible is extremely thickened in cross-section (pachyglossous)

Table 3

Data matrix for 20 selected Pleistocene and Recent cervid species, 3 outgroup artiodactyls, and 122 skeletal characters used in the parsimony analysis (PAUP 4.0).

format equate: a = 0+2; b = 0+1

Femur

The caput and the great trochanter of each femur were not connected with the diaphyses, while the distal epiphyses had just begun to fuse, indicating an age of less than three years. The

location and development of the muscle attachments (cha. 48) on the femur can be used to assign specimens to particular species in adult individuals (Pfeiffer 1999a), but could not be determined exactly here. As in *M. giganteus* and

Cervus, the diaphysis is rounded in cross section (cha. 50), the fossa intercondylaris is deep, and the distance of the condyles is small (cha. 52). The femur of *M. verticornis* from Bilshausen has a rough, but flattened facies poplitea (cha. 51) by contrast to *M. giganteus*, where the facies poplitea forms a rough, prominent tuberosity. This character is influenced by muscle development and individual age. Consequently, the relatively juvenile age of the individual from Bilshausen reflect the weaker expression of this feature.

Tibia

The proximal epiphyses are not fused to the diaphyses both of which were broken and subsequently reconstructed. The morphological characters of the proximal and distal ends of the tibia are similar to those of *Megaloceros giganteus*, thus the internal peak of the tuberculum intercondylare clearly projects beyond the external apex (cha. 53) (compare figure 8 in Pfeiffer 1999c) and, in particular, the development of the distal facets exhibits the derived character states found in *Megaloceros verticornis* and *M. giganteus* (cha. 56, 57, 58). The dorsal facet that contacts the malleolus lateralis is especially pronounced (cha. 57).

Calcaneus and talus

The calcaneus and talus of the right and left side yielded morphological data. The tuber calcanei

was not fused to the corpus calcanei. A small step between the edge of the sustentaculum tali and the articular facet of the calcaneus shaft (Pfeiffer 1999a: fig. 75a, 1a) represents a plesiomorphic character state (cha. 67).

The talus provides more information for the phylogenetic analysis, because all the characters utilised here can be studied in juvenile individuals. The morphology of the talus of *Megaloceros verticornis* is generally similar to that of *M. giganteus*. An important, derived character is an axially directed depression in the trochlea tali distalis (cha. 72).

Metatarsus III + IV

Both left and right metatarsals are complete, although their proximal part is reconstructed. The distal epiphyses were beginning to fuse with the diaphyses at the time of death. This ontogenetic stage is consistent with an individual age of two years. Due to the young age of the specimen the diaphyses of MT III + IV are not connected distally. Character states for the distal MT III + IV are similar to those for *Megaloceros giganteus* (Pfeiffer 1999c: fig. 9).

Phalanges

All phalanges of *M. verticornis* from Bilshausen could be studied. The epiphyses of the first and second phalanges, which fuse at the beginning of the second year in deer, are all completely fused

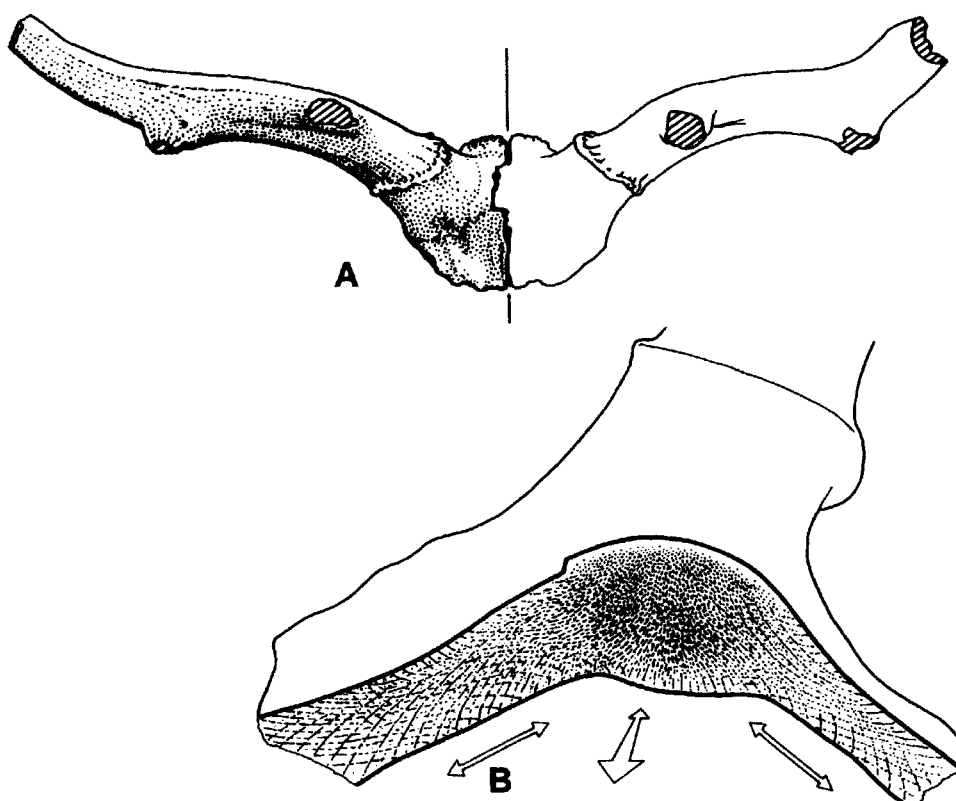


Fig. 4. A. Fragments of the skull and antler of an adult male of *Megaloceros verticornis* from Süßenborn. B. The frontal bones are particularly thick. The strategic alignment and distribution of trabecular bone is primarily related to the direction of normal loading. This orientation and the thickening of the frontals was also observed in the specimen from Süßenborn (IQW Süß 7117).

in the Bilshausen specimen. The first and second phalanges also have robust diaphyses and exhibit most morphological characters of *Megaloceros* (Pfeiffer 1999c: fig. 10).

Discussion and results

Many skeletal characters are influenced by ontogenetic growth patterns, sexual dimorphism, and functional adaptation, and may show high variability within a cervid species (Pfeiffer 1999a). An important problem is that characters of antlers and skulls of juvenile individuals of one species with a complex antler morphology can appear similar to characters of antlers of adult stages of other species. As an example *Cervus elaphus*, and *C. nippone* e.g. can have a three-point antler stage in juvenile individuals that is comparable to the antler stage of an adult of *Axis axis* (Table 2, cha. 92). In most species of deer the sutures of the skull are still almost visible in adult individuals, but are nearly completely erased in adult megalocerines (cha. 111). Juvenile megalocerines do not have pachygnathous mandibles as in most other species of deer, but they can be extremely pachygnathous in old individuals (Table 2, cha. 122). All antler- and skull characters in the data matrix (cha. 92–111, 122) are influenced by ontogenetic growth patterns. It is therefore extremely important to specify the character development in adult individuals of all species in the phylogeny reconstruction.

Megaloceros verticornis from Süßenborn and Voigtsdorf (Kahlke 1956, 1960, 1965, 1969) shows, that palmation clearly increases in older individuals. The enormous weight of these antlers resulted in special adaptations in cranial morphology. Bone material had to be added at the linea nucha, and this became a nuchal crest in older stags. Adult male deer with wide spread antlers therefore show an extreme thickening of the frontal bones between the pedicles. The strategic alignment and distribution of trabecular bone is primarily related to the principal direction of normal loading. This orientation and thickening of the frontals was observed in an adult male of *Megaloceros verticornis* from Süßenborn (Fig. 4). Similarly, an increase in antler development in *Alces latifrons* is related to the thickening of the frontals (Pfeiffer 1999b). Unfortunately, in the palaeontological literature the classification of the alcini is mainly based on adaptive characters (Azzaroli 1953, 1983, 1985, 1994). Breda (2001) discussed the skull charac-

ters of the alcini in more detail noting the structural adaptations made necessary by an increase of antler- and bodysize. The development of a nuchal crest, for example, could be observed in many cervid species with strong antlers, including *E. tegulensis*, *Cervus elaphus*, *Dama dama*, *M. giganteus*, and *Alces latifrons*. Such independently acquired characters seem to be highly homoplastic in cervids, and are difficult to use for determining phylogenetic relationships. This observation concords with the results of Scott & Janis (1993).

Results of the computer-aided cladistic analysis

The parsimony analysis (MP) using PAUP 4.0 resulted in a single most parsimonious tree (length 579, CI: 0.578). The robustness of the phylogeny was assessed using the bootstrap method (Fel-

Bootstrap

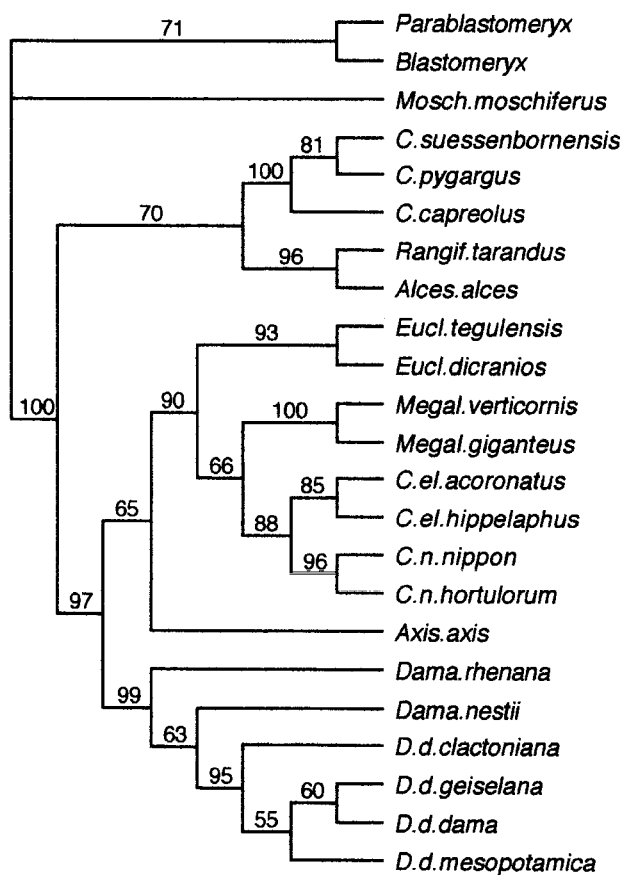


Fig. 5. Majority rule consensus tree, after 1000 bootstrap resamplings, describing the evolutionary relationships of 20 fossil and Recent cervids, and 3 outgroup artiodactyls as deduced from 122 skeletal characters. At each node the bootstrap percentage (BP) is given. One single most parsimonious tree (MP) was found with the same topology (length = 579, CI = 0.5872).

The monophly of *Megaloceros verticornis* and *M. giganteus* is well supported (BP = 100).

senstein 1985), and the maximum likelihood method (ML). The majority-rule consensus tree after 1000 bootstrap resamplings, describing the evolutionary relationships between 20 fossil and Recent cervids, and three outgroup artiodactyls based on a comparison of 122 skeletal characters obtain has the same topology as the MP tree (Fig. 5). The tree computed by the (ML) method differs only in the position of *Axis*, which is located in a clade with *Dama* in the ML analysis. At each node, the bootstrap percentage (BP) is given above the branch.

The family Cervidae is defined by 32 characters at the basal node of the MP tree, and there is strong support for cervid monophyly from the bootstrap values (BP = 100). This result agrees with the phylogenetic analysis computed from molecular data (Cronin et al. 1996, Douzery & Randi 1997, Randi et al. 1998). The subfamilies, Odocoileinae and Cervinae, occurred as monophyletic groups within the Cervidae. Fourteen characters (BP = 70) define the telemetacarpal

odocoileine deer, and 19 characters (BP = 97) define the plesiometacarpal Cervinae.

Within the Odocoileinae the genus *Capreolus* is considerably differentiated from the other taxa, with 19 characters defining its branch on the MP tree (BP = 100). *Capreolus suessenbornensis* (= *C. cusanoides* Kahlke 2001) from the late Lower Pleistocene of Untermaßfeld and the Middle Pleistocene of Germany (Mosbach, Miesenheim, Süßenborn) is nearly identical to its Recent relatives *C. capreolus* and *C. pygargus* in its skeletal characters. Three characters define the position of *C. capreolus* and the clade of *C. pygargus* and *C. suessenbornensis*, while one character defines *C. suessenbornensis*. These taxa differ only in body size and antler development, the diagnostic antler characters of *C. cusanoides* described by Kahlke (2001) can be included in the range of antler variation exhibited by *C. suessenbornensis* from Mosbach. Therefore *C. cusanoides* is assumed here to be a junior synonym of *C. suessenbornensis*.

Table 4

Metric data for preserved teeth and postcranial skeletal elements of *Megaloceros verticornis* from Bilshausen (measurements after v. d. Driesch 1976).

Upper/ lower molars	M¹	M²	M³		m₁	m₂
	sin	dex	sin	dex	sin	sin
max. length at crown-base in mm	26.0	29.0	(30.0)	29.5	29.0	29.0
max. width at crown-base in mm	29.5	30.0	(31.0)	29.5	29.5	18.5
Scapula				Femur		
height along the spine (HS in mm):			392.0	BP		143.5
greatest length at the processus articularis (GLP)	90.0			BD		116.5
width of the cavitas glenoidalis (BG)	61.5			KD		42.5
length of the cavitas glenoidalis (LG)			72.5			
Humerus				Tibia		
max. proximal width (BP)		117.0		BP		119.0
				BD		78.5
Radius and Ulna				Calcaneus and talus		
greatest length of the radius (GLR)			386.0	calcaneus		
max. proximal width of the radius (BP)	93.0			GL	176.0	81.8
max. distal width of the radius (BD)	80.5			GB	64.3	53.5
Metacarpus III+IV				Metatarsus III+IV		
greatest length (GL in mm)			343.0	GL		377.0
BP	65.0			BP		58.5
BD	65.5			BD		69.0
min. width of the diaphysis (KD)	39.5			KD		40.2
Phalanges						
	1st Ph.	2nd Ph.	3rd Ph.		posterior	
GL	80.0	61.0	76.0		1 st Ph.	
BP	34.0	33.5		85.5	2 nd Ph.	72.0
KD	27.5	26.5		36.8	3 rd Ph.	
max. height (GH)			48.0	26.5	26.9	
						46.0

The association of *Rangifer* in a clade with *Alces* (BP = 96) is in contrast to the results of a study by (Cronin et al. 1996) based on K-casein DNA-data. Both genera, for example, share a derived morphology of the lower p₄, and the clade is well supported by 25 characters in the analysis reported here. However, *Rangifer tarandus* is considerably differentiated from *Alces alces*: 24 characters define *R. tarandus*, while 20 characters support *A. alces*.

The plesiometacarpal deer split into a *Dama*-lineage, defined by 26 characters (BP = 99), and a clade consisting of the fossil genera *Eucladoceros*, *Megaloceros*, *Cervus* (fossil and Recent species), and the Recent species *Axis*, defined by 12 characters. The bootstrap value is low for this internal node (BP = 65, DI = +2).

As demonstrated by Pfeiffer (1999a) *Axis* shares many postcranial characters with the genus *Cervus*, and on the other hand, also with *Dama*, but locating *Axis* in a single clade with *Cervus*, *Eucladoceros*, and *Megaloceros*, involves 12 additional steps (by contrast to the 14 additional steps, necessary to unit *Axis* in a clade with *Dama*), and this is reflected in the relatively low consistency index of the data set (CI: 0.578).

Tree topology within the *Dama*-lineage reflects the evolution of this genus from the Plio-Pleistocene to the Holocene. In the Plio-Pleistocene *Dama rhenana* had evolved a three-point antler stage, followed in the Lower Pleistocene by *Dama nestii*, with a 4-point antler without palmation, and then, in the Middle Pleistocene to Recent times, of fallow deer with palmated antlers. Considering the rich skeletal material of the *Dama*-lineage it can be observed that more than one character state may occur in a single species for a particular character. Quite often, both apomorphic and plesiomorphic character states, may occur in the same species as a polymorphic character. Such apparently variable characters can yield important phylogenetic information. Within the *Dama*-lineage it was possible to follow the shift from a plesiomorphic character state that occurs with a high frequency in *Dama rhenana*, which lies at the basis of the lineage, to an apomorphic character state in the stratigraphically younger *Dama*-species (Pfeiffer 1999a, in press).

The clade including *Eucladoceros*, *Megaloceros* and *Cervus* is defined by 23 characters (BP = 90). Comparing this data in detail, the characters 2, 4, 5, 6 and 9 (concerning cervical vertebrae), 76, 77, 78, 82, 83, 84, 85, (concerning 1st and 2nd phalanges), 95, 96, (concerning ant-

lers), and 105, 107, (concerning the skull) all support this node. Except the Japanese sika deer *C. nippon nippon*, all taxa in this clade are robust cervids, with large and heavy antlers. The morphology of the cervical vertebrae is extremely influenced by the morphology and weight of the antlers, as demonstrated by Lengsfeld (1975) and Pfeiffer (1999a), and the phalanges need special adaptations to support the body weight (Pfeiffer 1999a, b). Therefore it should be taken into account that the high bootstrap value for this clade may be the result of homoplasy.

The clade including *Megaloceros* and *Cervus* is defined by 17 characters (BP = 66). In particular, the shared morphology of the tuberculum supraglenoidale of the scapula (cha. 14), the similar morphology of radius and ulna (cha. 26, 28, 29, 35), and the morphology of the upper M³ (cha. 118) was not observed in other plesiometacarpal deer genera, and seems to support their relationship.

As in other phylogeny reconstructions computed from molecular data (Cronin et al. 1996, Douzery & Randi 1997, Randi et al. 1998) the *Cervus* clade including red deer and sika deer is well supported (17 characters, BP = 88). Within *Cervus*, the East-Asian sika deer *Cervus nippon* (BP = 96) appears to have been distinct from the European *Cervus elaphus* since the Pliocene (BP = 85). A large group of consistent characters are present in *Cervus*, and appear to have persisted for a long time span. Moreover a study of bone material of *Pseudaxis grayi* Zdansky 1925 from Lower Pleistocene localities of the Shansi Basin in China shows evidence that *P. grayi* is an early, true member of *Cervus nippon* (Pfeiffer, in prep.).

Douzery & Randi (1997) calibrated divergence times on the basis of molecular data. In their study divergences of 3.3–7.1 Myr within the genus *Cervus* are postulated, and 0.4–2.5 Myr within *Cervus elaphus*.

Cervus elaphus was first identified in Europe from early Middle Pleistocene localities in Great Britain (Cromer Forest-bed, Lister 1996) and Germany (Voigtstedt, Süßenborn, Mosbach, Kahlke, 1956, 1960, 1965, Koenigswald & Heinrich 1999, Pfeiffer 1999a) represented by the fossil subspecies *C. elaphus acoronatus*. The antlers of *Cervus elaphus acoronatus* (= *Cervus acoronatus* Beninde 1937) from Mosbach always lack a crown in the distal part, although this species exhibits a nearly identical postcranial character set to that of extant individuals of *Cervus elaphus hippelaphus*. Three characters define *C. e.*

acoronatus, while five define the extant *C. elaphus hippelaphus*.

The monophyly of *Megaloceros verticornis* and *M. giganteus* is well supported (PB = 100, 27 steps), and these species share 15 postcranial character states do not occur in other plesiometacarpal deer species: the cranial facet of the 3rd and 4th cervical vertebrae (cha. 7), the shape of the cavitas glenoidalis of the scapula (cha. 12), the rounded scores in the fossa radialis of the humerus (cha. 21), the axially especially deep fossa olecrani (cha. 24), the development of the cranial facet of the radius (cha. 29, 30), character states of the distal tibia (cha. 56, 58), development of the proximal end of MC III + IV (cha. 61, 62), and the astragalus (cha. 72, 73). These characters seem to be diagnostic for giant deer, and support a close relationship between the two giant deer species which are combined in a single genus, *Megaloceros*, here.

Dama and *Megaloceros* clearly represent separate lineages within the main clade of plesiometacarpal deer, because they share relatively few postcranial skeletal character states. Moreover the topology of the MP tree supports the idea that the occurrence of palmate antlers in both genera must be the result of homoplasy.

Acknowledgements

I wish to thank Prof. Dr. D. Meischner and Prof. Dr. J. Schneider (Göttingen) for permission to study the giant deer from Bilshausen. Their kind support during my visits to Göttingen was of great help. Fig. 1 was provided by Prof. Meischner. I wish to thank Prof. Dr. H.-D. Kahlke (Weimar), Prof. Dr. W. v. Koenigswald (Bonn), Dr. G. Böhme, and Prof. Dr. H.-P. Schultz (Berlin) for kindly discussing issues covered in this study. I am very grateful to various scientists and curators who allowed me to study material in their care: Dr. M. Ade, Dr. W.-D. Heinrich (Berlin), Prof. Dr. A. v. d. Driesch (Munich), Dr. W. Eckloff (Lübeck), Dr. A. Feiler (Dresden), Dr. D. Heinrich (Kiel), Dr. R. Hutterer (Bonn), Dr. H. Jung (Mainz), PD Dr. R.-D. Kahlke (Weimar), Prof. Dr. D. Mania, (Jena), Dr. U. Scheer (Essen), Dr. G. Gruber (Darmstadt), Dr. G. Storch, Dr. G. Plodowski, Prof. Dr. F. Schrenck (Frankfurt), Dr. R. Ziegler, Dr. E. Heizmann (Stuttgart), Mr. E. Zenker (Wiesbaden), Dr. L. Abbazzi, Prof. Dr. D. Torre, Dr. L. Rook (Florence), Dr. L. Capasso Babato, Prof. Dr. C. Petronio (Rome), Prof. Dr. B. Engesser (Basel), Prof. Dr. C. Guerin, Dr. M. Fauré (Lyon), Dr. S. Stuenes (Uppsala), Dr. A. Sutcliffe, Dr. J. Hooker, Dr. A. Currant (London), Prof. Dr. E. Tchernov, Dr. R. Rabinovich (Jerusalem), Dr. R. Tedford (New York), Dr. J. d. Vos (Leiden). I am grateful to Dr. J. Dunlop, and Dr. D. Unwin (Berlin) for help in correcting the English text, and to Mr. J.-P. Mendau for producing Figs. 2 and 4, Mrs. E. Siebert (Berlin) for amending Fig. 1. I thank Prof. Dr. G. Arratia, Dr. D. Unwin, Prof. Dr. W. v. Koenigswald, and Dr. R. Ziegler for detailed reviews. This investigation was made possible by financial support from the Deutsche Forschungsgemeinschaft (DFG).

References

- Alessandri, G. de 1903. Sopra alcuni avanzi di cervidi pliocenici del Piemonte. — Atti della R. Accademia della Scienze Torino.
- Azzaroli, A. 1953. The deer of the Weybourne Crag and Forest bed of Norfolk. — Bulletin of the British Museum (Natural History), Geology **2**: 3–96.
- 1983. On the Quaternary and Recent Cervid Genera *Alces*, *Cervalces*, *Libralces*. — Bollettino Società Paleontologia Italiana **20**: 147–154.
- 1985. Taxonomy of Quaternary Alcini (Cervidae, Mammalia). — Acta Zoologica Fennica **170**: 179–180.
- 1994. Forest bed elks and giant deer revisited. — Zoological Journal of the Linnean Society **112**: 119–133.
- Azzaroli, A. & Mazza, P. 1992. On the possible origin of the Giant Deer genus *Megaceroides*. — Atti Accademia Lincei, Rendiconti Scienze Fisiche e Naturali (9th series) **3**: 23–32.
- Belgrand, E. 1869. Histoire générale de Paris. La Seine I: Basin parisien aux antéhistoriques **3**: 13. La Seine I. Basin parisien, planch. paléont. S.13, Taf. 18 ff.
- Beninde, J. 1937. Zur Naturgeschichte des Rothirsches. — Monographien der Wildsäugetiere **4**: 1–223.
- Bittmann, F. & Müller, H. 1996. The Kärlitz Interglacial site and its correlation with the Bilshausen sequence. In Turner, C. (ed.). The early Middle Pleistocene in Europe: 187–193. Balkema, Rotterdam.
- Bogaard, C. van den, Bogaard, P. van den & Schmincke, H.-U. 1989. Quartärgeologisch-tephrostratigraphische Neuauflnahme und Interpretation des Pleistozänprofils Kärlitz, F.R.G. — Eiszeitalter und Gegenwart **39**: 62–86.
- Breda, M. 2001. The holotype of *Cervalces gallicus* (Azzaroli, 1952) from Senéze (Haute-Loire, France) with nomenclatural implications and taxonomical-phylogenetic accounts. — Rivista Italiana di Paleontologia e Stratigrafia **107**(3): 439–449.
- Brookes, J. 1828. A Catalogue of the Anatomical and Zoological Museum Joseph Brookes, Esp., part 1: 61.
- Cronin, M. A., Stuart, R., Pierson, B. J. & Patton, J. C. 1996. K-casein gene phylogeny of higher ruminants (Pecora, Artiodactyla). — Molecular Phylogenetic Evolution **6**: 295–311.
- Dawkins, W. B. 1868. On a new species of fossil Deer from Clacton. — Quarterly Journal of the Geological Society of London **24**: 511–516.
- Douzery, E. & Randi, E. 1997. The Mitochondrial Control Region of Cervidae: Evolutionary Patterns and Phylogenetic Content. — Society for Molecular Biology and Evolution **14** (11): 1154–1166.
- Driesch, von den, A. 1976. Das Vermessen von Tierknochen aus vor- und frühgeschichtlichen Siedlungen. — Inst. Paläoanatomie, Domestikationsforschung und Geschichte der Tiermedizin Universität München: 1–114.
- Felsenstein, J. 1985. Confidence limits on phylogenies: an approach using the bootstrap. — Evolution **39**: 783–791.
- Freudenberg, W. 1914. Die Säugetiere des älteren Quartärs von Mitteleuropa. — Geologische und Paläontologische Abhandlungen **12** (4/5): 455–670.
- Geist, V. 1971. The relation of Social Evolution and Dispersal in ungulates during the Pleistocene, with Emphasis on the Old World Deer and the genus *Bison*. — Quaternary Research **1** (3): 283–315.
- 1987. On speciation in Ice Age mammals, with special reference to cervids and caprids. — Canadian Journal of Zoology **65**: 1067–1084.
- Goldfuß, G. A. 1820. Handbuch der Zoologie **2**: 20: 374.
- Gould, S. J. 1974. The origin and function of bizarre structures: antler size and skull size in the 'Irish elk', *Megaloceros giganteus*. — Evolution **28**: 191–220.
- Groves, C. P. & Grubb, P. 1987. Relationships of living deer. In Wemmer, C. M. (ed.). Biology and management of the Cervidae, pp. 21–59, Smithsonian Institution Press, Washington, D.C.

- Grüger, E., Jordan, H., Meischner, D. & Schlie, P. 1994. Mitteleistozäne Warmzeiten in Göttingen, Bohrungen Ottostraße und Akazienweg. — Geologisches Jahrbuch A **134**: 167–210.
- Habermehl, K. H. 1961. Die Altersbestimmung bei Haustieren, Pelztieren und beim jagdbaren Wild. — Parey, Hamburg und Berlin.
- Harmer, F. 1889. On a specimen of *Cervus belgrandi* (Lartet) (*C. verticornis* Dawk.) from the Forest-Bed of East Anglia. -Transactions of the Zoological Society **15**: London.
- Heintz, E. & Poplin, F. 1981. *Alces carinatum* (Laugel, 1862) du Pléistocène de Saint-Prest (France). Systématique et évolution des Alcénés (Cervidae, Mammalia). — Quartärpaläontologie **4**: 105–122.
- Joleaud, L. 1914. *Cervus (Megaceroides) algericus* Leydekker, 1890. — Recueil des Notices et Mémoires de la Société Archéologique du Dép. De Constantine **5** (5): 1–67.
- Kahlke, H.-D. 1956. Die Cervidenreste aus den altpaleistozänen Ilmkiesen von Süßenborn bei Weimar. — Bd. 1: 62 S., Akademie-Verlag, Berlin.
- 1960. Die Cervidenreste aus den altpaleistozänen Sanden von Mosbach (Biebrich-Wiesbaden). — Abhandlungen der Deutschen Akademie der Wissenschaften, Klasse für Chemie, Geologie und Biologie **7**: 1–75.
 - 1965. Die Cervidenreste aus den Tonen von Voigtsdorf. — Paläontologische Abhandlungen A **2** (2/3): 379–425.
 - 1969. Die Cerviden-Reste aus den Kiesen von Süßenborn bei Weimar. — Paläontologische Abhandlungen A **3** (3/4): 547–610.
 - 2001. Neufunde von Cerviden-Resten aus dem Unterpleistozän von Untermaßfeld. — Monographien des Römisch-Germanischen Zentralmuseums Mainz **40** (2): 461–482.
- Kahlke, R.-D. 1994. Die Entstehungs-, Entwicklungs- und Verbreitungsgeschichte des oberpleistozänen *Mammuthus – Coelodonta* – Faunenkomplexes in Eurasien (Großsäuger). — Abhandlungen der Senckenbergischen naturforschenden Gesellschaft **546**: 1–164.
- Kishino, H. & Hasegawa, M. 1989. Evaluation of the maximum likelihood estimate of the evolutionary tree topologies from DNA sequence data, and the branching order in Hominoidea. — Journal of Molecular Evolution **29**: 170–179.
- Koenigswald, W. v. & Heinrich, W.-D. 1999. Mittelpaleistozäne Säugetierfaunen aus Mitteleuropa – der Versuch einer biostratigraphischen Zuordnung. — Kaupia **9**: 53–112.
- Laugel, A. 1862. La faune de Saint-Prest, près Chartres (Eure-et-Loir). — Bulletin Société Géologique de France 2. Ser. **19** (1861–1862): 709–718.
- Lengsfeld, K.-P. 1975. Über den formenden Einfluß des Cervidengewebs auf Hinterhaupt und erste Halswirbel. — Dissertation Institut für Haustierkunde, Universität Kiel.
- Lister, A. M. 1984. Evolutionary and ecological origins of British deer. — Proceedings of the Royal Society of Edinburgh **82B**: 205–229.
- 1987. *Megaloceros* Brookes, 1828 (Mammalia, Artiodactyla): proposed emendation of the original spelling. — Bulletin of Zoological Nomenclature **44** (4): 255–256.
 - 1993. The stratigraphical significance of deer species in the Cromer Forest-bed Formation. — Journal of Quaternary Science **8**: 95–108.
 - 1994. The evolution of giant deer, *Megaloceros giganteus* (Blumenbach). — Zoological Journal of the Linnean Society **112**: 65–100.
 - 1996. The stratigraphical interpretation of large mammal remains from the Cromer Forest-bed Formation. In Turner, C. (ed.). The early Middle Pleistocene in Europe, pp. 25–44, Balkema, Rotterdam.
- Lydekker, R. 1890. On a Cervine Jaw from Algeria. — Proceedings of the Zoological Society of London for the year **1890**: 602–604.
- Meischner, D. 1995. Black Shales Models. — III EPA Workshop, Dotternhausen.
- Meischner, D. & Schneider, J. 1967. 500000 Jahre alter Steppenhirsch gefunden. — Deutsche Jägerzeitung **22**: 870–872.
- Moullade, E. 1886. Note sur une nouvelle espèce de daim fossile. — Mém. Soc. Agr. Sci. H. te Loire **4**: 304–306.
- Müller, H. 1965. Die pollenanalytische Neubearbeitung des Interglazial-Profil von Bilshausen (Unter-Eichsfeld). — Geologisches Jahrbuch **83**: 327–352.
- Newton, E. T. 1882. The Vertebrata of the Forest bed Series of Norfolk and Suffolk. — Memoirs of the Geological Survey of English Wales. HMSO, London.
- Owen, R. 1842. Report on British Fossil Mammalia. — Reports of the British Association, p. 237.
- Pfeiffer, T. 1999a. Die Stellung von *Dama* (Cervidae, Mammalia) im System plesiometacarpaler Hirsche des Pleistozäns — Phylogenetische Rekonstruktion — Metrische Analyse. — Courier Forschungsinstitut Senckenberg **211**: 1–218.
- 1999b. *Alces latifrons* (Johnson, 1874) (Cervidae, Mammalia) aus den jungpleistozänen Kiesen der Oberrheinebene. — Neues Jahrbuch für Paläontologie, Abhandlungen **211** (3): 291–327.
 - 1999c. The Morphological Distinction of Limb Bones of *Alces latifrons* (Johnson, 1874) and *Megaloceros giganteus* (Blumenbach, 1799). — Kaupia, Darmstädter Beiträge zur Naturgeschichte **9**: 113–126.
 - in press. The position of *Dama* (Cervidae, Mammalia) in the system of fossil and living deer from Europe — Phylogenetic analysis based on skeletal characters. — Quaternaire.
- Pomel, A. 1892. Sur deux ruminants de l'époque n°lithique en Algérie: *Cervus pachygenis* et *Antilope maupasi*. — C.R. Acad. Sc. Paris, **CXV**: 213.
- Portis, A. 1920. Elenco delle specie di cervicomi fossili in Roma e attorno a Roma. — Bollettino della Società Geologica Italiana **39**: 132–139.
- Randi, E., Mucci, N., Pierpaoli, M. & Douzery, E. 1998. New phylogenetic perspectives on the Cervidae (Artiodactyla) are provided by the mitochondrial cytochrome b gene. — Proceedings of the Royal Society of London B **265**: 793–801.
- Rieck, W. 1983. Damwildalter-Merkblatt. In Schalenwild-ausschuß des Deutschen Jagdschutz-Verbandes e.V. (ed.), 3. Aufl. S. 1–7, Hoffmann, Mainz.
- Schmidt, H. 1930. Ein Skelett von *Alces latifrons* aus der Gegend von Göttingen. — Paläontologische Zeitschrift **12**: 135.
- 1934. Ein Skelett vom Riesenelch. — Forschungen und Fortschritte **10** (15): 198–199.
- Scott, K. M. & Janis, C. M. 1993. Relationships of the Ruminantia (Artiodactyla) and an analysis of the characters used in ruminant taxonomy. In Szalay, F. S., Novacek, M. J. & Mc Kenna, M. C. (eds). Mammal Phylogeny: Placentalia, pp. 282–302, Springer, New York.
- Soergel, W. 1927. *Cervus megaceros mosbachensis* n. sp. und die Stammesgeschichte der Riesenhirse. — Abhandlungen der Senckenbergischen Naturforschenden Gesellschaft **39**: 375–505.
- Strimmer, K. & von Haeseler, A. 1996. Quartet puzzling: a quartet maximum-likelihood method for reconstructing tree topologies. — Molecular Biology and Evolution **13**: 964–969.
- Swofford, D. L. 1998. "PAUP*. Phylogenetic Analysis Using Parsimony (*and other methods)." Version 4. Sinauer Associates, Sunderland, MA.
- Thenius, E. 1958. Geweihjugendstadien des eiszeitlichen Riesenhirses, *Megaloceros giganteus* (Blum.) und ihre phylogenetische Bedeutung. — Acta Zoologica Cracoviensia **2** (30): 707–721.
- Zdansky, O. 1925. Fossile Hirsche Chinas. — Palaeontologia Sinica C **2** (3): 1–94.